Performance and Microbial Community Analysis of an Electrobiofilm Reactor Enhanced by Ferrous-EDTA

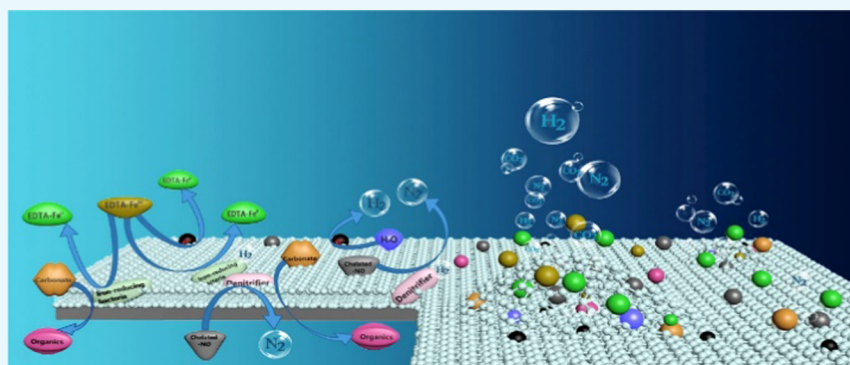Nan Liu, Ying-ying Li, Du-juan Ouyang, Chang-yong Zou, Wei Li,* Ji-hong Zhao, Ji-xiang Li, Wen-juan Wang,* and Ja-jun Hu

ACCESS | Metrics & More | Article Recommendations

ABSTRACT: The biological reduction of ferrous ethylenediaminetetraacetic acid (EDTA-Fe^{II}-NO and EDTA-Fe^{III}) is an important process in the integrated electrobiofilm reduction method, and it has been regarded as a promising alternative method for removing NO$_x$ from industrial boiler flue gas. EDTA-Fe^{II}-NO and EDTA-Fe^{III} are crucial substrates that should be biologically reduced at a high rate. However, they inhibit the reduction processes of one another when these two substrates are presented together, which might limit further promotion of the integrated method. In this study, an integrated electrobiofilm reduction system with high reduction rates of EDTA-Fe^{II}-NO and EDTA-Fe^{III} was developed. The dynamic changes of microbial communities in the electrobiofilms were mainly investigated to analyze the changes during the reduction of these two substrates under different conditions. The results showed that compared to the conventional chemical absorption-biological reduction system, the reduction system exhibited better performance in terms of resistance to substrate shock loading and high microbial diversities. High-throughput sequencing analysis showed that *Alicycliphilus*, *Enterobacteriaceae*, and *Raoultella* were the dominant genera (>25% each) during the process of EDTA-Fe^{II}-NO reduction. *Chryseobacterium* had the ability to endure the shock loading of EDTA-Fe^{III}, and the relative abundance of *Chryseobacterium* under abnormal operation conditions was up to 30.82%. *Ochrobactrum* was the main bacteria for reducing nitrate by electrons and the relative abundance still exhibited 16.11% under shock loading. Furthermore, higher microbial diversity and stable reactor operation were achieved when the concentrations of EDTA-Fe^{II}-NO and EDTA-Fe^{III} approached the same value (9 mmol·L^{-1}).

1. INTRODUCTION

As primary pollutants, nitrogen oxides (NO$_x$) not only directly affect human health but also combine with ozone and hydrocarbons to form photochemical smog in the troposphere.[1,2] In 2017, a total of 1258.8 × 10^4 t of NO$_x$ were emitted in China, according to the official data from the China National Bureau of Statistics.[3] However, during the outbreak of coronavirus (COVID-19) in February 2020, NASA and the European Space Agency (ESA) detected a significant decrease in airborne nitrogen dioxide (NO$_2$) over China. NO$_x$ emissions are related to industrialization in China,[4] and it is crucial to limit the release of NO$_x$ into the atmosphere.

For decades, the main anthropogenic source of NO$_x$ has been emissions from industrial boilers (kilns).[5,6] Some

technologies have been introduced for controlling flue gas from boilers (kilns) and reducing the release of NO$_x$, such as selective catalytic reduction (SCR), low-NO$_x$ burners, absorption, adsorption, and selective noncatalytic reduction (SNCR).[7,8] However, these methods can have a high cost, low removal efficiency, and cause secondary pollution.[9] The
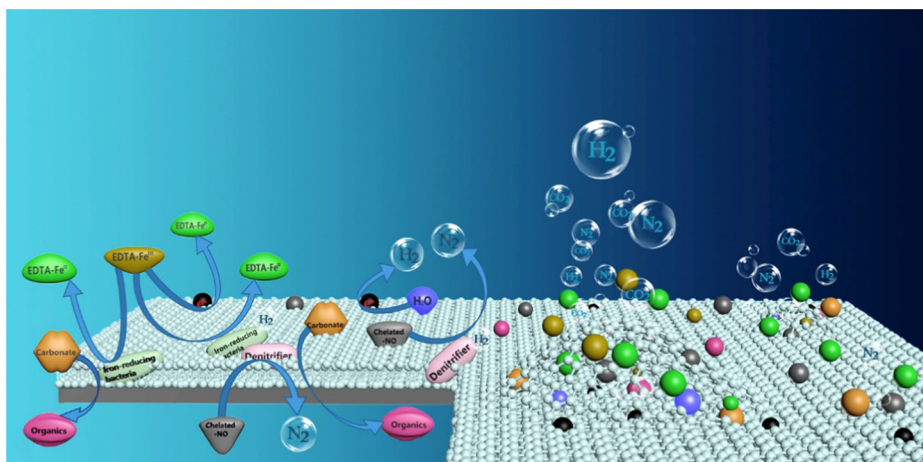
Figure 1. Principle of electrobiofilm processing.

biological treatment of industrial flue gas for NO_x removal was proposed in the 1980s as a low-cost and environmentally sustainable approach, and related studies have focused mainly on isolating denitrifying bacteria and improving biological reactors.[10,11] Wang et al.[12] studied denitrifying bacteria in bioreactors for landfill leachate treatment and found that the main bacteria in the bioreactor varied with changes in the hydraulic loading. Sposob et al.[13] analyzed the microbial communities involved in autotrophic sulfide denitrification with changes in temperature and found that *Thauera* sp. and *Alicycliphilus* sp. were predominant at 25 °C. Xing et al.[14] studied the microorganisms involved in the micro-electrolysis and autotrophic denitrification processes by high-throughput sequencing and found that β-, γ-, and α-*Proteobacteria* were the dominant genera. However, biological approaches have been limited by their low efficiency, which is caused by the low solubility of NO in liquid and the higher proportion of NO in NO_x from flue gas.[15,16] Therefore, a new integrated technology has been developed that combines complex absorption processes with biological reduction.[6,17] Ferrous ethylenediaminetetraacetic acid (EDTA-Fe^{II}) had been reported to rapidly form complexes with NO, which resolves the issues associated with the low gas−liquid mass transfer efficiency of NO.[18] An electrobiofilm was subsequently introduced and has been demonstrated to further strengthen the regeneration rate of EDTA-Fe^{II},[19] as it not only forms complexes with NO to generate EDTA-Fe^{II}-NO but also oxidizes into EDTA-Fe^{III} by oxygen in the flue gas (approximately 9% content in the flue gas in industrial boilers).[20]

Therefore, the biological regeneration of EDTA-Fe^{II} was believed to be a key step to allow the greater application of this method.[21] This is depicted in Figure 1, which describes the principle of the electrobiofilm-integrated method for NO_x removal. The electrobiofilm method integrates the advantages of both electrochemical and complex absorption-bioreduction (CABR) processes. This method offers bacteria with two categories of electron donors, carbon sources and currents, thereby enhancing the diversity and activity of the microorganisms.[22]

Several microorganisms have been screened for L-Fe^{III} and L-Fe^{II}-NO reduction with high efficiency, where L represents complexes of citrate or EDTA.[23,24] Zhang et al.[25] studied the microbial communities in CABR-integrated systems by the polymerase chain reaction-denaturing gradient gel electro-

phoresis (PCR-DGGE) method and found that *Pseudomonas* sp. was the dominant microorganism related to the NO_x removal in the biofilm. Li et al.[26] also analyzed the microbial communities in CABR-integrated systems by high-throughput sequencing and found that the dominant denitrifying bacteria varied from anaerobic to facultative anaerobic and aerobic denitrifying bacteria with an increase in the inlet oxygen loading. Wang et al.[27] analyzed the microbial community structure of the BTF-ABR-integrated system by the real-time polymerase chain reaction and high-throughput sequencing method. The results showed that the cooperation of denitrifying bacteria and iron-reducing bacteria in the system was the key to the stable and efficient removal of NO_x and the regeneration of EDTA-Fe^{II} simultaneously. High-throughput sequencing, also referred to as "deep sequencing" technology, involves the parallel sequencing of millions of molecules at a time, allowing rapid, detailed, and comprehensive analysis of the transcriptome and genome of a species or a microbial community.[28] High-throughput sequencing has a more rapid response, higher accuracy, and larger reaction scale than the previously widely used applications, such as PCR-DGGE,[29] and has become an efficient research method in the field of molecular biology.[30] However, electrobiofilm-integrated systems are typical multiphase complexes, and their microbial communities have not yet been studied. Illuminating the microbial communities of such systems could allow for a better understanding of the EDTA-Fe^{II} regeneration mechanism. Additionally, the stability and capacity for long-term operations are crucial indicators for evaluating a bioreactor.[21] The sensitivity of the microbial system is an important factor affecting the stable operation of a bioreactor.[20] Microorganisms are sensitive to changes in environmental factors, such as temperature, process conditions, and load changes.[31] However, promoting the biofilm diversity in an electrobiofilm system can improve resistance to shock loading of NO_x and EDTA-Fe^{III}.

The objective of this study is to describe the key factors affecting the activities of an electrobiofilm and evaluate the changes in microbial communities of electrobiofilm-integrated systems under shock loadings of the main absorption product EDTA-Fe^{II}-NO and the oxidation product EDTA-Fe^{III} by the molecular biotechnology of high-throughput sequencing. Furthermore, the changes of dominant strains under different conditions and the regeneration of EDTA-Fe^{II} under different

electron donor combinations are analyzed. Finally, approaches to achieving stable operation of electrobiofilm-integrated systems were explored based on the variation of the microbial communities. This work will identify the biological mechanism of EDTA-Fe^{II} regeneration in the bio-electrochemical system, discuss the optimal control mechanism of microbial activities in this kind of system, and provide theoretical reference for engineering applications on NO$_x$ removal in the future.

2. RESULTS AND DISCUSSION

2.1. Biofilm Formation in the Reactor. The formation of an electrobiofilm is vital in achieving the efficient reduction of EDTA-Fe^{II}-NO and EDTA-Fe^{III} in the reactor. Batch experiments were conducted with a solution containing up to 2 g·L^{-1} glucose and 18 mmol total iron at the startup of the electrobiofilm reactor. The biofilm started becoming visible on the surface of the cathodes from the tenth day. EDTA-Fe^{II}-NO was gradually added after 22 days, followed by repeated batch reduction until its concentration was equal to the initial EDTA-Fe^{III} concentration.

As shown in Figure 2, when the reduction efficiency of EDTA-Fe^{II} became stable at around 80%, it is considered that
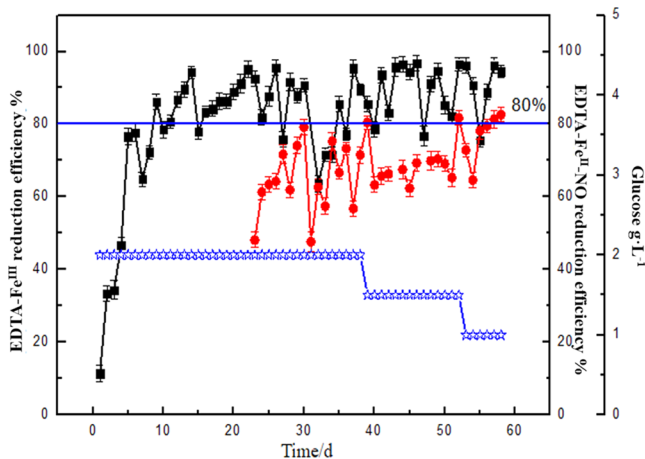

Figure 2. Reduction efficiency of different EDTA-Fe^{II}-NO and EDTA-Fe^{III} concentrations (total Fe = 18 mmol, I = 20 mA, U = 12 V, initial glucose = 0.2 g·L^{-1}, liquid flow rate = 1.2 L·min^{-1}, pH = 6.7–6.9) (solid black box: EDTA-Fe^{II}-NO concentrations; solid red circle: EDTA-Fe^{III} concentrations; and blue star: glucose concentrations).

the reactor has adapted to a certain ratio of substrate combinations. The current increased gradually as an electron donor after the 38th day (Table 1). That is, part of glucose (carbon source) was replaced by the current. The composition of the electron donor was changed to adapt the microorganisms to a carbon source (glucose) concentration of 1 g·L^{-1}. At the end of the eighth week, the biofilm on the cathode was highly dense, according to field emission scanning electron

Table 1. Conditions of Electron Donors in Different Stages of Biofilm Formation

stages	current (mA)	glucose (mg·L^{-1})
7-1	10	2000
7-2	15	1500
7-3	20	1000

microscopic (FESEM) images, as shown in Figure 3. The efficiency of EDTA-Fe^{II} regeneration increased from 12 to 94% after 55 days. During the stable operation of the reactor, the CO$_2$ produced at the anode dissolved in the liquid phase and formed a CO$_2$–HCO$_3^{2-}$ system that had a buffering effect on the pH value, such that the pH value in the reactor generally remained between 6.7 and 6.9. By contrast, the EDTA-Fe^{II} regeneration efficiency reported by Gao et al.[22] was 76–85% at the end of the 90-day domestication period. Overall, the sequential biofilm formation method could accelerate the domestication of microorganisms and biofilm formation due to the negative effects of EDTA-Fe^{II}-NO on the activities of microorganisms in electrobiofilm systems[32] and difficulties in the cultivation of microbial systems that relied on an electrical current as an electron donor.

2.2. Optimization of Electron Donor Combination. Electrical currents and carbon sources (glucose) are the crucial electron donors in electrobiofilm treatment and primarily impact the EDTA-Fe^{II} regeneration rate. In our earlier studies, the respective influence of each electron donor on the EDTA-Fe^{II} regeneration rate was discussed. The carbon sources were more important donors for EDTA-Fe^{II} regeneration than the electrical current. To investigate the interactions between current and glucose and their influences on the EDTA-Fe^{II} regeneration rate, a factorial analysis of the effects under different electron donor combinations was also performed. When both variables influence the experimental results, these can be used as a function to evaluate the interactive effects of cathode electrons and glucose during EDTA-Fe^{II} regeneration.

The results obtained under different currents and carbon sources were used to develop a prediction model equation using Design-Expert software, which is as follows

$$V = +0.80 - 0.014 \cdot I + 0.28 \cdot G + 7.42 \cdot 10^{-3} \cdot I \cdot G + 0.024 \cdot I^2 + 0.020 \cdot G^2$$

where V is the regeneration rate of EDTA-Fe^{II} (mmol·L^{-1}·h^{-1}), I is the applied current (mA), and G is the glucose concentration (g·L^{-1}). The P-value of the model obtained by factorial analysis was 0.0063 ($P \leq 0.05$), indicating that the obtained model was reliable and statistically significant.

The coefficient of G was positive, suggesting that the effect of glucose is positive, and could promote the regeneration of EDTA-Fe^{II}. Meanwhile, the coefficient of I was negative, suggesting that the regeneration of EDTA-Fe^{II} was reduced with an increased current. The $I \cdot G$ coefficient was positive, indicating that the interaction between the two electron donors could promote EDTA-Fe^{II} regeneration (either or both of the EDTA-Fe^{II}-NO and EDTA-Fe^{III} reduction). Glucose acted as an essential organic carbon source for the growth of microorganisms and was an electron donor during the EDTA-Fe^{III} and EDTA-Fe^{II}-NO reduction. The hydrogen produced by the cathode electrons could be used by microorganisms in situ. Thus, these two processes promoted the regeneration of EDTA-Fe^{II}.[32,3332,33] It had been speculated that the microbial activity contributed more to the regeneration of EDTA-Fe^{II}, while the current promoted other aspects of the electrobiofilm system. Therefore, the biofilm mechanism in this system needs to be better understood.

By comparing the actual value obtained from the experiment with the predicted value obtained from the prediction equation under the operating conditions of a 20 mA current and glucose
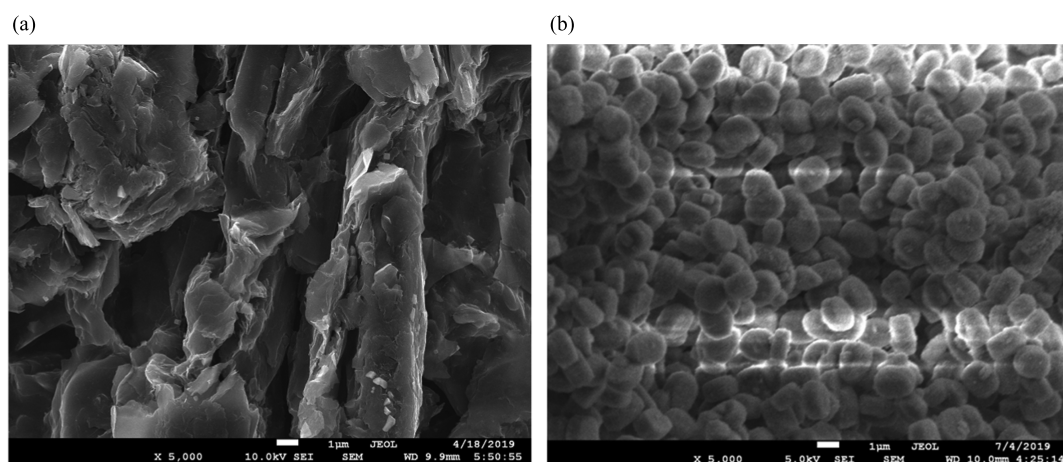
Figure 3. FESEM images of (a) the electrode before biofilm formation and (b) the electrobiofilm after full growth (×5000).

content of 1000 mg·L^{-1}, it was found that the actual and predicted values were well correlated (i.e., coefficient of correlation (R^2) of 0.84; Figure 4). Additionally, according to
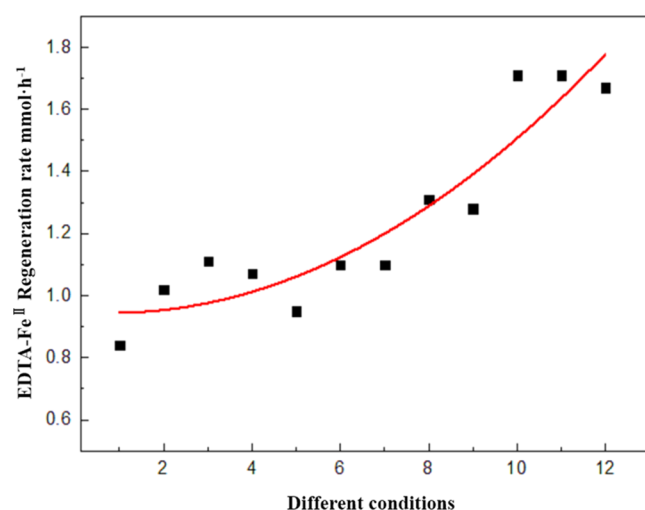

Figure 4. Prediction curve of the EDTA-Fe^{II} regeneration rate ([EDTA-Fe^{II}-NO] = 9 mmol, [EDTA-Fe^{III}] = 9 mmol, U = 12 V, G = 1 g·L^{-1}, liquid rate = 1.2 L·min^{-1}, pH = 6.7−6.9).

Table 2, when the current was 20 mA and the glucose content was 1000 mg·L^{-1}, the prediction equation gave the smallest deviation with the experimental EDTA-Fe^{II} regeneration rates. Moreover, when the concentration of the electron donor exceeded a certain value, the EDTA-Fe^{II} regeneration rate generally stayed stable. Therefore, considering the reduction efficiency and long-term stability of the reactor, this kind of electron donor combination was thought to be optimal and more beneficial for maintaining stable operation of the system.

2.3. Reduction of EDTA-Fe^{II}-NO and EDTA-Fe^{III} under Different Substrate Concentration Ratios. It has been confirmed that EDTA-Fe^{II}-NO and EDTA-Fe^{III} can inhibit one another during the reduction of either substrate.[21] Therefore, to ensure the stable, long-term operation of the electrobiofilm reactor, the EDTA-Fe^{II}-NO and EDTA-Fe^{III} reduction efficiencies were studied under operating conditions that covered a range of different concentrations. The reactor was operated for no less than 14 days under each concentration ratio.

Table 2. Factorial Analysis of Different Electron Donor Combinations

batch	electron donor glucose (mg·L^{-1})	current (mA)	EDTA-Fe^{II} regeneration rate (mmol·h^{-1}) experimental value	predictive value
1	200	10	0.96	1.02
2	200	20	1.02	0.98
3	200	60	1.11	0.96
4	300	10	1.07	1.09
5	300	20	1.11	1.06
6	300	60	1.10	1.25
7	500	10	1.10	1.04
8	500	20	1.31	1.22
9	500	60	1.28	1.21
10	1000	10	1.71	1.67
11	1000	20	1.71	1.70
12	1000	60	1.67	1.65

As shown in Figure 5, the reduction efficiencies of both EDTA-Fe^{II}-NO and EDTA-Fe^{III} became optimal under a concentration ratio of 1:1. Moreover, the reactor remained steady during the operating conditions presented in Figure 5. There was no decrease in the reduction efficiencies of EDTA-Fe^{II}-NO and EDTA-Fe^{III} at high EDTA-Fe^{II}-NO concentrations (i.e., the concentration ratio of 3:1). Both EDTA-Fe^{II}-NO and EDTA-Fe^{III} were fully reduced after 10 h of daily operation. However, the reduction efficiencies of EDTA-Fe^{II}-NO appeared to be lower (i.e., 70%), under a concentration ratio of 1:5. A high concentration of EDTA-Fe^{III} can inhibit the activities of microorganisms in the electrobiofilm, as the actual reduction of EDTA-Fe^{II}-NO at an initial EDTA-Fe^{II}-NO concentration of approximately 3−4 mmol·L^{-1} was much lower than that under other substrate concentration ratios. However, the EDTA-Fe^{II}-NO reduction efficiency improved as the EDTA-Fe^{III} concentration decreased. Therefore, microbial activity is considered critical during the reduction of EDTA-Fe^{II}-NO, in that EDTA-Fe^{III} can inhibit the activity of the EDTA-Fe^{II}-NO-reducing bacteria. This indicates that high concentration of chelated NO would have toxic effects on substrate-reducing bacteria, thus inhibiting the reduction of EDTA-Fe^{III}. Previous studies by our research team found that EDTA-Fe^{II}-NO was easier to be reduced than EDTA-Fe^{III} in an electrode biofilm reactor under the same experimental conditions, and the two substrates have a competitive
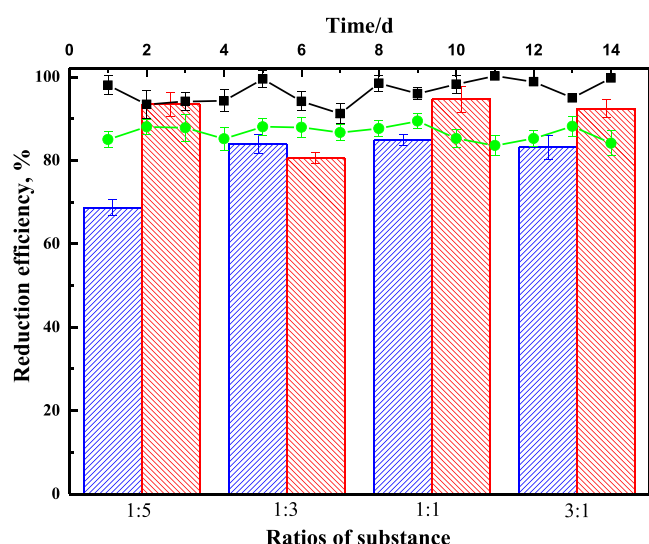
Figure 5. Reduction efficiencies of EDTA-Fe^{II}-NO and EDTA-Fe^{III} under different substrate ratios ([EDTA-Fe^{II}-NO] = 9 mmol, [EDTA-Fe^{III}] = 9 mmol I = 20 mA, U =12 V, liquid rate = 1.2 L·min^{-1}, pH = 6.7−6.9) (solid blue box: EDTA-Fe^{II}-NO; solid red box: EDTA-Fe^{III}; solid green circle: EDTA-Fe^{II}-NO under 1:1; and solid black box: EDTA-Fe^{III} under 1:1).

relationship during the reduction process. In the presence of EDTA-Fe^{II}-NO, the reduction rate of EDTA-Fe^{III} was initially inhibited, especially when the concentration of EDTA-Fe^{II}-NO was 6 mmol·L^{-1}, and the reduction of EDTA-Fe^{III} was almost quit in the first 3 h.

2.4. Microbial Community Analysis. The α-diversity can reflect the number of species in microbial communities, while the species abundance and diversity of communities can be evaluated through a series of statistical analysis of molecular biological indices.[43] The coverage index indicates the extent to which the coverage of various sample libraries reflects the reliability of the sequencing results.[34] As shown in Table 3, the coverage value of the samples under all experimental conditions is 1, implying that the α-diversity index is reliable for sequencing and the samples were all well tested.

Table 3. Statistics of the α-Diversity Index

sample	Shannon index	ACE index	chao1 index	coverage
biofilm formation	3.341	35.243	34.5	1
1:5	3.623	35	35	1
1:3	3.459	19	19	1
1:1	3.5	44	44	1
3:1	2.769	48.601	47.333	1
abnormal operation	3.208	42	42	1

2.4.1. Microbial Community during Biofilm Formation. As mentioned above, the biofilm growth on the cathode was observed to be dense. Moreover, higher amounts of cocci than bacilli grew, and this was captured in FESEM images using a magnification of 5000×. To further investigate the distribution of bacteria, the samples from the electrobiofilm were analyzed by 16S rDNA high-throughput sequencing.

Ten of the most abundant microbial species after electro-biofilm formation are shown in Figure 6. *Raoultella* occurred at abundances of 27% and has a certain ability in terms of denitrification.[35] *Dysgonomonas* is a type of autotrophic EDTA-
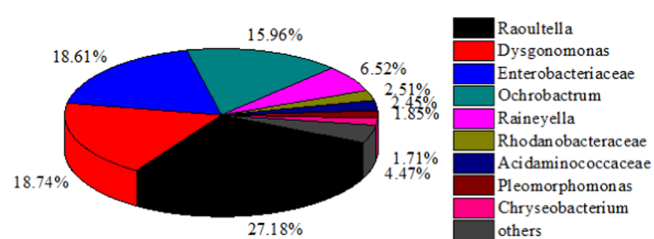

Figure 6. Microbial community under the conditions of biofilm formation.

Fe^{III}-reducing bacteria,[36] while *Ochrobactrum* can catalyze nitrate reduction by electrons.[37] *Chryseobacterium* occurred at relatively low abundances but may also be involved in EDTA-Fe^{III} reduction.[32] *Raineyella* and *Enterobacteriaceae* are also denitrifying bacterial genera.[33] The mature microbial community in the electrobiofilm changed greatly from that of the inoculated sludge from the wastewater treatment plant under an anaerobic environment in which the growth of autotrophic or heterotrophic anaerobic denitrifying bacteria was promoted. However, further studies are required to clarify whether the bacteria mentioned above can reduce chelated NO (EDTA-Fe^{II}-NO). Nonetheless, microbial species diversity greatly benefits the long-term stable operation of the reactor.[24]

2.4.2. Microbial Community under Different Substrate Concentration Ratios. Variations in the substrate concentrations had a great impact on the distribution of bacteria in the reactor. Therefore, the characteristics of the microbial communities in the electrobiofilm under different substrate concentrations were investigated using the high-throughput sequencing, as shown in Figure 7. First, the EDTA-Fe^{III} reduction efficiency reached 95% under EDTA-Fe^{II}-NO and EDTA-Fe^{III} ratios of 1:5, 1:3, and 1:1, as shown in Figure 5. Both *Dysgonomonas* and *Chryseobacterium* were present under these ratios and were also predominant with abundances ranging from 10 to 30%, respectively. Both of these bacteria can reduce EDTA-Fe^{III}.[36,38−41] The reduction efficiency of EDTA-Fe^{II}-NO exceeded 80% in ratios of 1:3, 1:1, and 3:1, and the reduction efficiency of EDTA-Fe^{III} decreased to 80%, which is almost equal to that of EDTA-Fe^{II}-NO under the ratio of 1:3. Therefore, the two types of reducing bacteria appeared to exhibit similar competitiveness toward the electron donors at this ratio, resulting in a decrease in the abundance of the microbial community. This was also indicated by the ACE and Chao1 index results presented in Table 3. *Falsochrobactrum*, *Ochrobactrum*, and *Raineyella* were presumed to be the dominant denitrifying-bacteria genera during the EDTA-Fe^{III} reduction process.[33,34,37] *Alicycliphilus* is a genus of denitrifying bacteria that can reduce NO_2^- to N_2,[35] and its abundance increased apparently with increases in the EDTA-Fe^{II}-NO concentration. It is inferred that *Alicycliphilus* is the main denitrifying bacteria for chelated-NO reduction. It has been confirmed that a high concentration of NO has a toxic effect not only on EDTA-Fe^{III}-reducing bacteria but also on EDTA-Fe^{II}-NO-reducing bacteria.[35] When the ratio of EDTA-Fe^{II}-NO and EDTA-Fe^{III} was 3:1, the abundance of *Enterobacteriaceae*, a genus of denitrifying bacteria, increased notably to approximately 28% and was considered to be one of the predominant bacteria for EDTA-Fe^{II}-NO reduction. Additionally, a new genus of denitrifying bacteria, i.e., *Raoultella*, was observed in the electrobiofilm and accounted for approximately 30% of the community.[35] In summary, high microbial
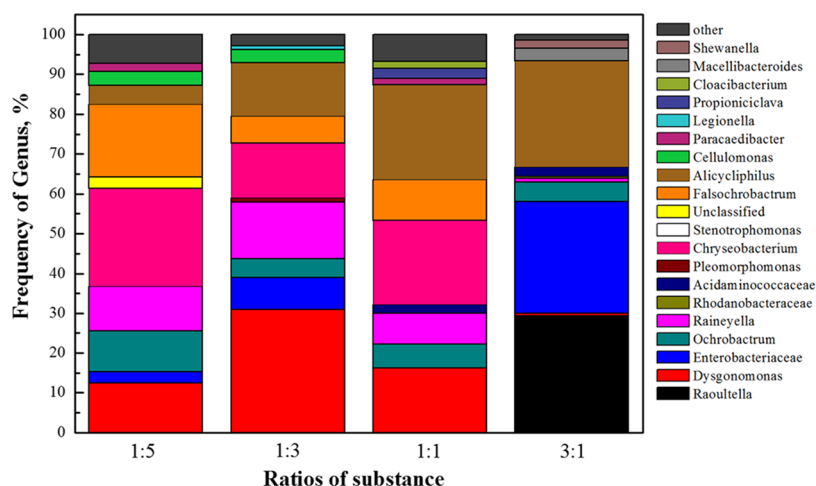
Figure 7. Microbial communities at different ratios of the substrate.

diversity and stable reactor operation could be achieved, when the concentrations of EDTA-Fe^{II}-NO and EDTA-Fe^{III} were similar. The microbial communities cultivated in the electro-biofilm reactor studied here differed significantly from those of the enhanced CABR system studied by Li et al.,[24] and no autotrophic bacteria were observed without current in the CABR system as a carbon source. This is mainly because the hydrogen produced by cathode electrons could be utilized by microorganisms in situ and promoted the growth of autotrophic reducing bacteria in the presence of an external current (Figure 8).
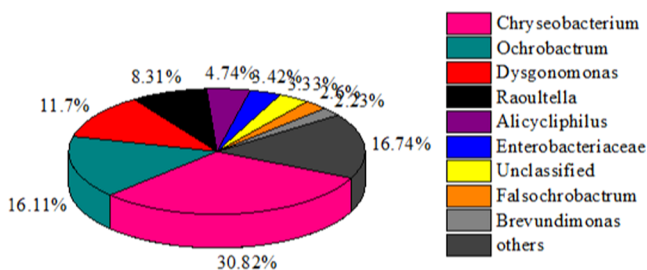

Figure 8. Microbial community of unsteady operation.

2.4.3. Evaluation of the Microbial Community under Abnormal Operation Conditions. To study the shock-loading resistance of the reactor and its corresponding microbial diversity, the initial concentration of EDTA-Fe^{II}-NO was increased to 6 mmol, while the EDTA-Fe^{III} concentration remained at 12 mmol. After 21 days of operation, the EDTA-Fe^{II}-NO and EDTA-Fe^{III} reduction efficiencies decreased, as shown in Figure 9. The reduction of EDTA-Fe^{II}-NO decreased by approximately 15%, while that of EDTA-Fe^{III} decreased slightly by approximately 8%. At this time, the biofilm on the cathode differed significantly from that of the reactor during stable operation, as is apparent from the FESEM images shown in Figure 10a,b, respectively. By comparing the microbial distribution at the same magnification, it can be seen that the cocci were reduced while the agglomeration phenomenon intensified under low reactor efficiency. The microbial community is further illuminated in Figure 8.

The abundance of *Chryseobacterium* was significantly higher than that in Figure 6, indicating that the EDTA-Fe^{III}-reducing bacteria on the electrobiofilm could resist the shock loading.
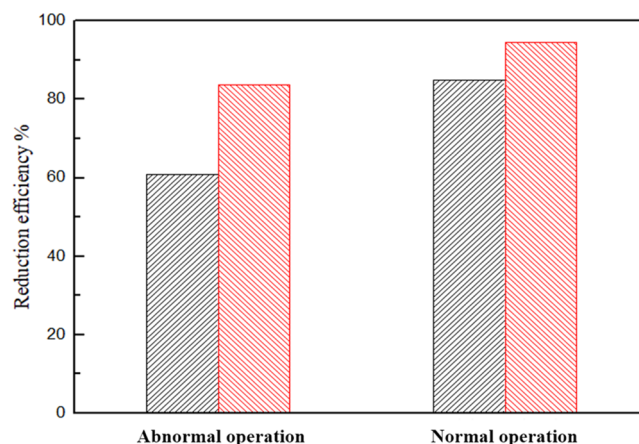

Figure 9. Comparison of reduction efficiencies of EDTA-Fe^{II}-NO and EDTA-Fe^{III} under different operation conditions ([EDTA-Fe^{II}-NO] = 6 mmol, [EDTA-Fe^{III}] = 12 mmol, liquid rate = 1.2 L·min^{-1}, pH = 6.7−6.9, U = 12 V, G = 1 g·L^{-1}) (solid black box: EDTA-Fe^{II}-NO and solid red box: EDTA-Fe^{III}).

However, the abundance of *Dysgonomonas* decreased to 11%, indicating that autotrophic EDTA-Fe^{III}-reducing bacteria were sensitive to variation in shock loading. Moreover, according to Figure 7, the presence of EDTA-Fe^{II}-NO may have inhibited the growth of *Dysgonomonas*. The proportion of *Ochrobactrum* in the microbial community exhibited better stability under shock loading.[37] According to Figure 7, the reduction of EDTA-Fe^{II}-NO exceeded 80% under the EDTA-Fe^{II}-NO and EDTA-Fe^{III} ratios of 1:3, 1:1, and 3:1, while *Alicycliphilus*, *Enterobacteriaceae*, and *Raoultella* were presumed to be the dominant genera involved in EDTA-Fe^{II}-NO reduction (>25% each). However, their abundance apparently decreased to 3−9% each, as shown in Figure 8, thereby inhibiting the ability of the electrobiofilm reactor to reduce EDTA-Fe^{II}-NO.

By comparing the microbial communities under all of the conditions in this study, the ACE and Chao1 indices were found to be suitable at describing the amount of microbial growth[34] and gave values that were higher at substrate concentration ratios of 1:1 and 3:1. This indicates that denitrifying bacteria genera were generally more abundant than EDTA-Fe^{III}-reducing bacteria in the electrobiofilm reactor. The distribution of species on the electrobiofilm under ratios of 1:1 and 1:5 was well balanced, while it was not under a ratio
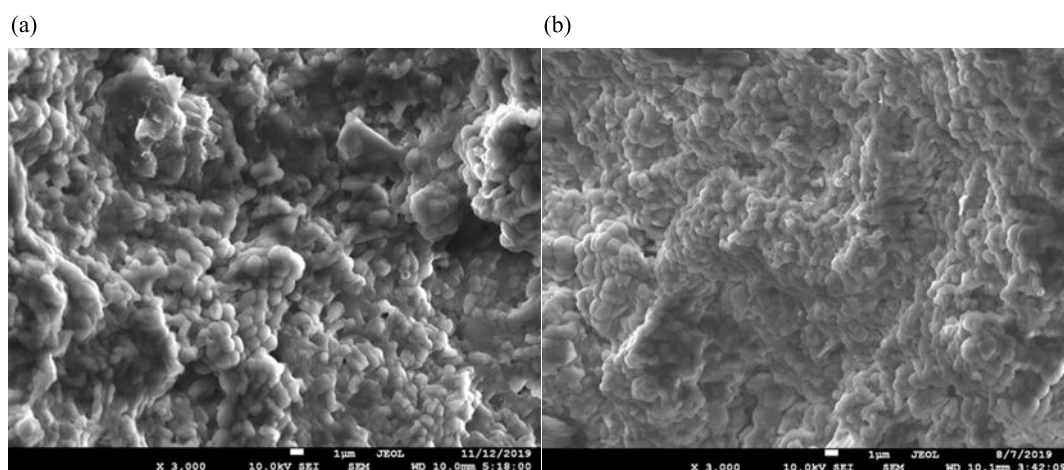
Figure 10. FESEM images of different operation conditions of the reactor (×3000). (a) FESEM image of reduction efficiencies of EDTA-Fe^{II}-NO and EDTA-Fe^{III} declined. (b) FESEM image of stable operation of the reactor.

of 3:1 and abnormal operating conditions, according to the Shannon index. The growth of the same genera of denitrifying bacteria was relatively concentrated. Therefore, high microbial diversity and stable reactor operation could be achieved when the concentrations of EDTA-Fe^{II}-NO and EDTA-Fe^{III} were almost equal.

3. CONCLUSIONS

This study revealed the key influencing factors and the structure of the microbial community in the reduction of EDTA-Fe^{II}-NO and EDTA-Fe^{III} by an electrobiofilm system. Microbial activity was considered to be critical in the reduction of EDTA-Fe^{II}-NO, and a rich microbial diversity in an electrobiofilm reactor is important in resisting shock loading and ensuring long-term stable operation. As an EDTA-Fe^{III}-reducing bacteria, *Chryseobacterium* can endure shock loading well. *Dysgonomonas* is a type of autotrophic EDTA-Fe^{III}-reducing bacteria that is sensitive to variation in shock loading. *Ochrobactrum*, which can reduce nitrate using electrons, is more stable under shock loading. *Alicycliphilus, Enterobacteriaceae*, and *Raoultella*, accounting for approximately 80% of the electrobiofilm community, are likely to be the dominant genera involved in EDTA-Fe^{II}-NO reduction, suggesting that the chelated NO-reducing bacteria were predominant in this system. Therefore, higher microbial diversity and stable reactor operation could be achieved when the concentrations of EDTA-Fe^{II}-NO and EDTA-Fe^{III} became comparable.

4. MATERIALS AND METHODS

4.1. Apparatus Setup. All experiments were conducted in an electrode biofilm reactor consisting of a cylindrical reactor (internal diameter/height: 0.12/0.2 m) with an effective working volume of 1.5 L.[19] An anode rod was placed in the center of the reactor, surrounded by four evenly spaced cathode rods. All of the graphite electrodes were Φ6 × 10 mm in size. Approximately half of the reactor's volume was filled with graphite particles, which provided proliferation of the attachment area for the biofilm, and were loaded in an orderly manner into the reactor. The total mass of graphite particles was 1380 g, while the total specific surface area was 533.33 m^2·g^{-1}. The internal space of the reactor was then sealed to create an anaerobic environment. Power was supplied to the reactor

using a stabilized direct current system (FPS-325DU, ZUUC Co., China).[22]

4.2. Medium and Microorganisms. The basal medium was prepared with the following composition (per liter): 2000 mg of D-glucose, 600 mg of KH$_2$PO$_4$, 140 mg of Na$_2$SO$_3$, 200 mg of MgCl$_2$, and 10 800 mg of NaHCO$_3$. The trace elements (per liter) were as follows: 40 mg of CaCl$_2$, 9.6 mg of CoCl$_2$, 39.6 mg of MnCl$_2$·4H$_2$O, 10 mg of CuSO$_4$·5H$_2$O, 8.8 mg of Na$_2$MoO$_4$·2H$_2$O, 7.6 mg of NiCl$_2$·6H$_2$O, 0.56 mg of H$_3$BO$_4$, and 4 mg of ZnCl$_2$.[4242]

All of the gases used in this study (NO (5% in N$_2$, v/v and N$_2$ (99.999%))) were purchased from Zhengzhou Yuanzheng Gas Products Co., China, while all reagents were supplied by Zhengzhou Yi-Zhi-Duo Reagent Chemistry Co., China, all of which were of analytical reagent grade.

The microorganisms used to inoculate the reactor were obtained from the sludge of a facultative anaerobic reactor in a local sewage treatment plant of Zhengzhou, China. The sludge—sewage mixture was collected and the supernatant was discarded. The reactor was then inoculated with 50 mL of the concentrated sludge to conduct the experiments.

4.3. Preparation of EDTA-Fe^{II}, EDTA-Fe^{II}-NO, and EDTA-Fe^{III}. Chelated EDTA-Fe^{III} solutions were prepared by mixing equimolar proportions of FeCl$_3$·6H$_2$O and Na$_2$EDTA·2H$_2$O with deionized water. Chelated EDTA-Fe^{II} solutions were prepared under anoxic conditions by mixing equimolar proportions of FeSO$_4$·7H$_2$O and Na$_2$EDTA·2H$_2$O.[15] EDTA-Fe^{II}-NO was then prepared by introducing NO (g) into EDTA-Fe^{II} solution, while the pH was adjusted to 5 using a NaOH solution.[19] The pH was adjusted during the experiment with 2 mmol·L^{-1} NaOH or HCl solution.

4.4. Determining Electron Donors for Optimizing EDTA-Fe^{II} Regeneration under Different Substrate Concentration Ratios. The biofilm was domesticated following the sequential batch method, while the culture medium in the reactor was changed daily. The culturing of EDTA-Fe^{II}-NO-reducing bacteria began after the culturing of EDTA-Fe^{III}-reducing bacteria had been completed. The concentrations of EDTA-Fe^{II}-NO and EDTA-Fe^{III} could be taken as indicators of the impacts of NO$_x$ or oxygen loads from the flue gas on the reactor, respectively. This experiment was designed to determine the main electron donor for EDTA-Fe^{II} regeneration and explore its impacts on microbial commun-

ities. Regarding the biofilm, the carbon source (glucose) and current were analyzed as electron donors for EDTA-Fe^{II} regeneration under different conditions. The general operating conditions during this study were maintained as follows: total iron content of 9−18 mmol, glucose of 1000−2000 mg·L$^{−1}$, current of 10−20 mA, and voltage of 12 V. The pH varied between 6.7 and 6.9 in the presence of a CO_2−$HCO_3^{2−}$ buffering reagent. The volume of the solution was 1.5 L. Samples were collected at regular intervals to measure the EDTA-Fe^{II} content, pH value, and EDTA-Fe^{II}-NO content. The operation of the bioreactor was described in terms of the EDTA-Fe^{II} regeneration efficiency (η) and elimination capacity (q_e), which were evaluated using the following equations.[20]

$$\eta = \frac{C_0 - C_e}{C_0} \times 100\% \tag{1}$$

$$q_e = \frac{V(C_0 - C_e)}{m} \tag{2}$$

where C_e and C_0 denote the inlet and outlet EDTA-Fe concentrations (mmol·L$^{−1}$) in the absorbent, respectively; V is the absorbent volume (L); and m is the absorbent weight (g).

4.5. Biological Community Analysis. Biofilm samples were obtained via ultrasonic vibration, purified to allow the microscopic analysis of the surface of the fillers, and then observed using a field environmental scanning electron microscope (FESEM, Philips Model XL30). Microbial samples were collected from the biofilm during biofilm formation under normal and abnormal reactor operations.

To conduct metagenomics analysis, 16S rDNA gene high-throughput sequencing was performed on the amplified V_3−V_4 region.[43] The process was as follows: sample preparation → DNA extraction and detection → PCR amplification → product purification → gene library preparation and detection → Miseq sequencing.[44] A Sangon Biotech DNA isolation kit was used to extract DNA from each sample. The PCR amplification conditions were as follows: TransStart Buffer (2.5 μL), TransStart Taq DNA (0.5 μL), dNTPs (2 μL), the primers (2 × 1 μL), template DNA (20 ng), and ddH$_2$O (25 μL). The sequencing data were processed by first filtering the low-quality original data, followed by obtaining a valid sequence for cluster analysis after the removal of the chimeric sequence, which then followed the taxonomic analysis of the representative sequence of each cluster to determine the species distribution of each sample,[45] Alpha diversity index (ADI) analysis was conducted to determine the species richness based on the results of the ACE, Chao1, and Shannon index analysis, and the community structure was analyzed at each classification level based on taxonomic information.[46]

4.6. Analytical Methods. The concentrations of ferrous ions and chelated NO in the solution were determined by 1,10-phenanthroline colorimetry at 510 and 438 nm, respectively, using a spectrophotometer (752N, Shanghai, China).[47] The pH was measured using a Mettler Toledo pH electrode (LE438-2M IP 67, Shanghai, China). The samples were treated with bacterial filters prior to measurement.

All of the data reported in this study are the mean values of duplicate or triplicate experiments and were analyzed using Origin 8.0 and Design-Expert 8.0. The confidence level used in this study is 95%, while the probability of achieving different results was determined based on the t-distribution.

■ **AUTHOR INFORMATION**

Corresponding Authors

Wei Li − *Key Laboratory of Biomass Chemical Engineering of Ministry of Education, Institute of Industrial Ecology and Environment, College of Chemical and Biological Engineering, Zhejiang University, Hangzhou 310027, P. R. China;* orcid.org/0000-0002-6216-9499; Email: w_li@zju.edu.cn

Wen-juan Wang − *Shanghai Advanced Research Institute, Chinese Academy of Sciences, Shanghai 201210, P. R. China;* Email: wangwenjuan@sari.ac.cn

Authors

Nan Liu − *Key Laboratory of Pollution Treatment and Resource, China National Light Industry; Collaborative Innovation Center of Environmental Pollution Control and Ecological Restoration, Department of Material and Chemical Engineering, Zhengzhou University of Light Industry, Zhengzhou 450001 Henan, P. R. China;* orcid.org/0000-0003-4364-065X

Ying-ying Li − *Key Laboratory of Pollution Treatment and Resource, China National Light Industry; Collaborative Innovation Center of Environmental Pollution Control and Ecological Restoration, Department of Material and Chemical Engineering, Zhengzhou University of Light Industry, Zhengzhou 450001 Henan, P. R. China*

Du-juan Ouyang − *Key Laboratory of Pollution Treatment and Resource, China National Light Industry; Collaborative Innovation Center of Environmental Pollution Control and Ecological Restoration, Department of Material and Chemical Engineering, Zhengzhou University of Light Industry, Zhengzhou 450001 Henan, P. R. China*

Chang-yong Zou − *Key Laboratory of Pollution Treatment and Resource, China National Light Industry; Collaborative Innovation Center of Environmental Pollution Control and Ecological Restoration, Department of Material and Chemical Engineering, Zhengzhou University of Light Industry, Zhengzhou 450001 Henan, P. R. China*

Ji-hong Zhao − *Henan Radio & Television University, Zhengzhou 450001, P. R. China*

Ji-xiang Li − *Shanghai Advanced Research Institute, Chinese Academy of Sciences, Shanghai 201210, P. R. China; University of Chinese Academy of Sciences, Beijing 100049, P. R. China*

Ja-jun Hu − *Shanghai Key Laboratory of Bio-Energy Crops, School of Life Sciences, Shanghai University, Shanghai 200444, P. R. China*

Complete contact information is available at:
https://pubs.acs.org/10.1021/acsomega.0c05876

Author Contributions

Material preparation and background analysis were performed by J.-h.Z. and J.-j.H. The manuscript-specific experimental design and operation, and experimental data processing were performed by C.-y.Z., Y.-y.L., and D.-j.O. Data analysis was performed by N.L. and J.-x.L. The background and experimental direction of the manuscript were performed by Wei Li and Wen-juan Wang. The first draft of the manuscript was written by Nan Liu. All authors have commented on previous versions of the manuscript and have read and approved the final manuscript.

◼ REFERENCES

(1) Kita, K.; Kawakami, S.; Miyazaki, Y.; Higashi, Y.; Kondo, Y.; Nishi, N.; Koike, M.; Blake, D. R.; Machida, T.; Sano, T.; et al. Photochemical production of ozone in the upper troposphere in association with cumulus convection over Indonesia. *J. Geophys. Res. Atmos.* **2017**, *53*, 1−4.

(2) Zhang, S.-H.; You, J.-P.; Chen, H.; Ye, J.-X.; Cheng, Z.-W.; Chen, J.-M. Gaseous toluene, ethylbenzene, and xylene mixture removal in a microbial fuel cell: Performance, biofilm characteristics, and mechanisms. *Chem. Eng. J.* **2020**, *386*, No. 123916.

(3) National Bureau of Statistics. Nitrogen oxides emission data in 2017. 2019. Web. 6 June, 2020. https://data.stats.gov.cn/easyquery.htm?cn=C01&zb=A0C05&sj=2019.

(4) Yu'e, L.; Erda, L. Emissions of N_2O, NH_3 and NO_x from fuel combustion, industrial processes and the agricultural sectors in China. *Nutr. Cycling Agroecosyst.* **2000**, *57*, 99−106.

(5) Shi, Y.; Xia, Y.-F.; Lu, B.-H.; Liu, N.; Zhang, L.; Li, S.-J.; Li, W. Emission inventory and trends of NOx for China, 2000-2020. *J. Zhejiang Univ., Sci., A* **2014**, *15*, 454−464.

(6) Zhang, C.-Y.; Zhao, J.-K.; Sun, C.; Li, S.-J.; Zhang, D.-X.; Guo, T.-J.; Li, W. Two-stage chemical absorption-biological reduction system for NO removal: system start-up and optimal operation mode. *Energy Fuels* **2018**, *32*, 7701−7707.

(7) Barman, S.; Philip, L. Integrated system for the treatment of oxides of nitrogen from flue gases. *Environ. Sci. Technol.* **2006**, *40*, 1035−1041.

(8) Guo, R.-T.; Hao, J.-K.; Pan, W.-G.; Yu, Y.-L. Liquid Phase Oxidation and Absorption of NO from Flue Gas: A Review. *Sep. Sci. Technol.* **2015**, *50*, 310−321.

(9) Cheng, G.; Zhang, C.-X. Desulfurization and Denitrification Technologies of Coal-fired Flue Gas. *Pol. J. Environ. Stud.* **2018**, *27*, 481−489.

(10) Ottengraf, S. P. P. Biological systems for waste gas elimination. *Trends Biotechnol.* **1987**, *5*, 132−136.

(11) Flanagan, W. P.; Apel, W. A.; Barnes, J.-M.; Lee, B. D. Development of gas phase bioreactors for the removal of nitrogen oxides from synthetic flue gas streams. *Fuel* **2002**, *81*, 1953−1961.

(12) Wang, J.; Yuan, Q.; Xie, B. Temporal dynamics of cyanobacterial community structure in Dianshan Lake of Shanghai, China. *Ann. Microbiol.* **2015**, *65*, 105−113.

(13) Sposob, M.; Cydzik-Kwiatkowska, A.; Bakke, R.; Dinamarca, C. Temperature-induced changes in a microbial community under autotrophic denitrification with sulfide. *Process Biochem.* **2018**, *69*, 161−168.

(14) Xing, W.; Li, D.-S.; Li, J.-L.; Hu, Q.-Y.; Deng, S.-H. Nitrate removal and microbial analysis by combined micro-electrolysis and autotrophic denitrification. *Bioresour. Technol.* **2016**, *211*, 240−247.

(15) Lu, B.-H.; Jiang, Y.; Cai, L.-L.; Liu, N.; Zhang, S.-H.; Li, W. Enhanced biological removal of NOx from flue gas in a biofilter by Fe(II)Cit/Fe(II)EDTA absorption. *Bioresour. Technol.* **2011**, *102*, 7707−7712.

(16) Fan, L.-R.; Huang, S.-B.; Yang, J.; Zhang, Y.-Q. Separating and Studying of the Aerobic Denitrifying Bacteria from Biofilter. *Microbiology* **2008**, *35*, 679−684.

(17) Zhang, S.-H.; Chen, H.; Xia, Y.-F.; Liu, N.; Lu, B.-H.; Li, W. Current advances of integrated processes combining chemical absorption and biological reduction for NO_x removal from flue gas. *Appl. Microbiol. Biotechnol.* **2014**, *98*, 8497−8512.

(18) Gambardella, F.; Alberts, M. S.; Winkelman, J. G. M.; Heeres, E. J. Experimental and Modeling Studies on the Absorption of NO in Aqueous Ferrous EDTA Solutions. *Ind. Eng. Chem. Res.* **2005**, *44*, 4234−4242.

(19) Mi, X.-H.; Gao, L.; Zhang, S.-H.; Cai, L.-L.; Li, W. A new approach for Fe(III)EDTA reduction in NO_x scrubber solution using bio-electro reactor. *Bioresour. Technol.* **2009**, *100*, 2940−2944.

(20) Chen, M.-X.; Zhou, J.-T.; Zhang, Y.; Wang, X.-J.; Shi, Z.; Wang, X.-W. Fe(III)EDTA and Fe(II)EDTA-NO reduction by a sulfate reducing bacterium in NO and SO_2 scrubbing liquor. *World J. Microbiol. Biotechnol.* **2015**, *31*, 527−534.

(21) van der Maas, P.; van der Brink, P.; Utomo, S.; Klapwijk, B.; Lens, P. NO removal in continuous $BioDeNO_x$ reactors: Fe(II)EDTA regeneration, biomass growth, and EDTA degradation. *Biotechnol. Bioeng.* **2006**, *94*, 575−584.

(22) Gao, L.; Mi, X.-H.; Zhou, Y.; Li, W. A pilot study on the regeneration of ferrous chelate complex in NOx scrubber solution by a biofilm electrode reactor. *Bioresour. Technol.* **2011**, *102*, 2605−2609.

(23) Liu, N.; Jiang, J.-L.; Cai, L.-L.; Li, W. Characterization and optimization of Fe(II)Cit-NO reduction by *Pseudomonas* sp. *Environ. Technol.* **2011**, *32*, 1947−1953.

(24) Li, W.; Li, M.-F.; Zhang, L.; Zhao, J.-K.; Xia, Y.-F.; Liu, N.; Li, S.-J.; Zhang, S.-H. Enhanced NO_x removal performance and microbial community shifts in an oxygen-resistance chemical absorption−biological reduction integrated system. *Chem. Eng. J.* **2016**, *290*, 185−192.

(25) Zhang, S.-H.; Chen, H.; Xia, Y.-F.; Zhao, J.-K.; Liu, N.; Li, W. Re-acclimation performance and microbial characteristics of a thermophilic biofilter for NO_x removal from flue gas. *Appl. Microbiol. Biotechnol.* **2015**, *99*, 6879−6887.

(26) Li, W.; Zhang, L.; Liu, N.; Shi, Y.; Xia, Y.-F.; Zhao, J.-K.; Li, M.-F. Evaluation of NO Removal from Flue Gas by a Chemical Absorption-Biological Reduction Integrated System: Complexed NO Conversion Pathways and Nitrogen Equilibrium Analysis. *Energy fuels* **2014**, *28*, 4725−4730.

(27) Wang, Y.-L.; Li, J.-J.; Huang, S.-B.; Huang, X.-Z.; Hu, W.-Z.; Pu, J.; Xu, M.-Y. Evaluation of NO_x removal from flue gas and Fe(II)EDTA regeneration using a novel BTF-ABR integrated system. *J. Hazard. Mater.* **2021**, *415*, No. 125741.

(28) Schuster, S. C. Next-generation sequencing transforms today's biology. *Nat. Methods.* **2008**, *5*, 16−18.

(29) Mutlu, B. K.; Ozgun, H.; Ersahin, M. E.; Kaya, R.; Eliduzgun, S.; Altinbas, M.; Kinaci, C.; Koyuncu, I. Impact of salinity on the population dynamics of microorganisms in a membrane bioreactor treating produced water. *Sci. Total Environ.* **2019**, *646*, 1080−1089.

(30) Wang, J.-Y.; Rong, H.-W.; Zhang, C.-S. Evaluation of the impact of dissolved oxygen concentration on biofilm microbial community in sequencing batch biofilm reactor. *J. Biosci. Bioeng.* **2018**, *125*, 532−542.

(31) Xia, Y.-F.; Chen, H.; Zhao, J.-K.; Li, W. Shifts of Biomass and Microbial Community Structure in Response to Current Densities in a Biofilm Electrode Reactor for NO_x Removal. *Energy fuels* **2019**, *33*, 5415−5421.

(32) Xia, Y.-F.; Zhao, J.-K.; Li, M.-F.; Zhang, S.-H.; Li, S.-J.; Li, W. Bioelectrochemical Reduction of Fe(II)EDTA-NO in a Biofilm Electrode Reactor: Performance, Mechanism, and Kinetics. *Environ. Sci. Technol.* **2016**, *50*, 3846−3851.

(33) Li, W.; Xia, Y.-F.; Zhao, J.-K.; Liu, N.; Li, S.-J.; Zhang, S.-H. Generation, Utilization, and Transformation of Cathode Electrons for Bioreduction of Fe(III)EDTA in a Biofilm Electrode Reactor Related to NO_x Removal from Flue Gas. *Environ. Sci. Technol.* **2015**, *49*, 4530−4535.

(34) Bunge, J.; Willis, A.; Walsh, F. Estimating the Number of Species in Microbial Diversity Studies. *Annu. Rev. Stat. Appl.* **2014**, *1*, 427−445.

(35) Li, P.; Wang, Y.-J.; Zuo, J.-N.; Wang, R.; Zhao, J.; et al. Nitrogen Removal and N_2O Accumulation during Hydrogenotrophic Denitrification: Influence of Environmental Factors and Microbial Community Characteristics. *Environ. Sci. Technol.* **2017**, *51*, 870−879.

(36) Gupta, A. B. Thiosphaera pantotropha: A sulphur bacterium capable of simultaneous heterotrophic nitrification and aerobic denitrification. *Enzyme Microb. Technol.* **1997**, *21*, 589−595.

(37) Chen, S.-H.; Hu, M.-Y.; Liu, J.-J.; Zhong, G.-H.; Liu, Y.; Muhammad, R.; Han, H.-T. Biodegradation of beta-cypermethrin and 3-phenoxybenzoic acid by a novel Ochrobactrum lupini DG-S-01. *J. Hazard. Mater.* **2011**, *187*, 433−440.

(38) Su, J.-F.; Shao, S.-C.; Huang, T.-L.; Ma, F.; Zhang, K.; Zheng, S.-C.; et al. Isolation, identification, and algicidal activity of aerobic denitrifying bacterium R11 and its effect on Microcystis aeruginosa. *Water. Sci. Technol.* **2016**, *73*, 2600−2607.

(39) Pikuta, E. V.; Menes, R. J.; Bruce, A. M.; Lyu, Z.; Hoover, R. B.; Busse, H. J.; Lawson, P.-A.; Whitman, W.-B.; et al. Raineyella antarctica gen. nov. sp. nov. a novel psychrotolerant, D-amino acid utilizing anaerobe isolated from two geographic locations of the Southern Hemisphere. *Int. J. Syst. Evol. Microbiol.* **2016**, *66*, 5529−5536.

(40) Sun, L.-N.; Yao, L.; Gao, X.-H.; Huang, K.-H.; Bai, N.-L.; Liu, W.-G.; Chen, W. Falsochrobactrum shanghaiense sp. nov. isolated from paddy soil and emended description of the genus Falsochrobactrum. *Int. J. Syst. Evol. Microbiol.* **2019**, *69*, 778−782.

(41) Weelink, S. A. B.; Tan, N. C. G.; Broeke, H.; Langenhoff, A. A. M.; Gerritse, J.; Junca, H.; Stams, A. J. M.; et al. Isolation and characterization of Alicycliphilus denitrificans strain BC which grows on benzene with chlorate as the electron acceptor. *Appl. Environ. Microb.* **2008**, *74*, 6672−6681.

(42) Zhang, S.-H.; Mi, X.-H.; Cai, L.-L.; Jiang, J.-L.; Li, W. Evaluation of complexed NO reduction mechanism in a chemical absorption−biological reduction integrated NO_x removal system. *Appl. Microbiol. Biotechnol.* **2008**, *79*, 537−544.

(43) Reuter, J. A.; Spacek, D. V.; Snyder, M. P. High-Throughput Sequencing Technologies. *Mol. Cell.* **2015**, *58*, 586−597.

(44) Pantaleo, V.; Szittya, G.; Moxon, S.; Miozzi, L.; Moulton, V.; Dalmay, T.; Burgyan, J. Identification of grapevine microRNAs and their targets using high-throughput sequencing and degradome analysis. *Plant J.* **2010**, *62*, 960−976.

(45) Anders, S.; Pyl, P. T.; Huber, W. HTSeq-a Python framework to work with high-throughput sequencing data. *Bioinformatics* **2015**, *31*, 166−169.

(46) Hori, T.; Aoyagi, T.; Itoh, H.; Narihiro, T.; Azusa, O.; Suzuki, K.; Ogata, A.; Friedrich, M. W.; Conrad, R.; Kamagata, Y. Isolation of microorganisms involved in reduction of crystalline iron(III) oxides in natural environments. *Front. Microbiol.* **2015**, *6*, No. 386.

(47) Liu, N.; Lu, B.-H.; Zhang, S.-H.; Jiang, J.-L.; Cai, L.-L.; Li, W.; Yi, H. Evaluation of Nitric Oxide Removal from Simulated Flue Gas by Fe(II)EDTA/Fe(II)citrate Mixed Absorbents. *Energy Fuels* **2012**, *26*, 4910−4916.